

InsideBias: Measuring Bias in Deep Networks and Application to Face Gender Biometrics

Ignacio Serna, Alejandro Pea, Aythami Morales, Julian Fierrez
School of Engineering, Universidad Autonoma de Madrid, Spain
{ignacio.serna, alejandro.penna, aythami.morales, julian.fierrez}@uam.es

Abstract—This work explores the biases in learning processes based on deep neural network architectures through a case study in gender detection from face images. We employ two gender detection models based on popular deep neural networks. We present a comprehensive analysis of bias effects when using an unbalanced training dataset on the features learned by the models. We show how ethnic attributes impact in the activations of gender detection models based on face images. We finally propose InsideBias, a novel method to detect biased models. InsideBias is based on how the models represent the information instead of how they perform, which is the normal practice in other existing methods for bias detection. Our strategy with InsideBias allows to detect biased models with very few samples (only 15 images in our case study). Our experiments include 72K face images from 24K identities and 3 ethnic groups.

I. INTRODUCTION

Artificial Intelligence (AI) algorithms have an increasingly growing role in our daily lives. These algorithms influence now many decision-making processes affecting peoples lives in many important fields, e.g. social networks, forensics, health, and banking. For example, some companies already use AI to predict credit risk, and some US states run prisoner details through AI systems to predict the likelihood of recidivism when considering parole [1].

Face recognition algorithms are good examples of recent advances in AI. During the last ten years, the accuracy of face recognition systems has increased up to 1000x (it is probably the biometric technology with the greatest investment nowadays). These face recognition algorithms are dominated by Deep Neural Network architectures, which are trained with huge amounts of data with little control over what is happening during training (focused on performance maximization). As a result, we have algorithms with excellent performance but quite opaque.

This trend in AI (excellent performance + low transparency) can be observed not only in face biometrics, but also in many other AI applications as well [2]. At this point, and despite the extraordinary advances in recognition performance, factors such as the lack of transparency, discrimination, and privacy issues are limiting many AI practical applications. As an example of these increasing concerns, in May 2019, the Board of Supervisors of San Francisco banned the use of facial recognition software by the police and other agencies, and many others are considering or already have enacted legislation [3].

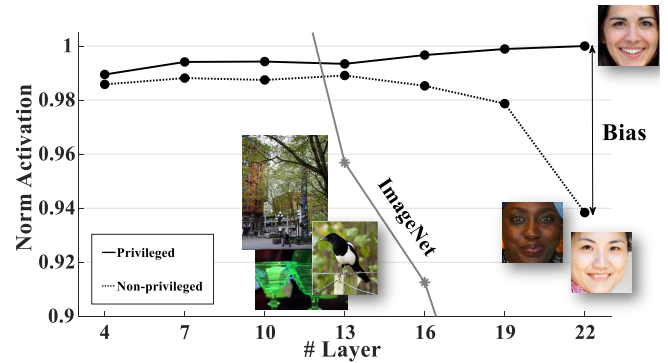


Fig. 1. Normalized overall activation observed through layers of a biased ResNet model trained for facial gender recognition. Overall activation for the images of a privileged group (continuous line), an underprivileged group (dotted line) and ImageNet (non-face images). The arrow on the right highlights the difference in activations obtained between privileged and underprivileged groups.

The number of published works pointing out the biases in the results of face recognition algorithms is large [4–7]. Among these works, a vast majority analyzes how biases affect the performances obtained for different demographic groups [3, 4, 6, 8–17]. However, only a limited number of works analyze how biases affect the learning process of these algorithms. In this work we use feature visualization techniques of deep models to generate a better understanding of biased learning. We will analyze two gender recognition models based on face images and how the ethnicity bias affects the learning process.

Given an input, the activations of the different neurons inside a neural network define the output of the network. Fig. 1 shows the difference in the overall activation of a gender recognition network for input face images from two different demographic groups. The figure shows the overall activations at different layers for face images of a privileged demographic group (caucasian female in this example), an underprivileged demographic group (black and asian females in this example), and images from a general purpose image classification database (ImageNet [18]). Privileged group refers to a demographic group prioritized during the training phase of the network with many more samples compared to underprivileged groups. The overall activation is measured for each image in each layer and then averaged across images of the same demographic group. Strong activations are usually

related with highly discriminant features [19]. In the figure, for the privileged group we can observe how the activations of the gender classification network are high for the first layers (focused on characterizing textures and colors) increasing slightly for the last layers (focused on the high level features related to the gender classification task). In comparison, for the underprivileged group the activations decrease significantly towards the final layers. These lower activations may be the cause of biased performances that result in unfair discrimination.

The contributions of this work are twofold:

- Comprehensive analysis of biased learning focused on the effects over the activation level of learned features in a database of 24,000 face images from 3 ethnic groups; demonstrating the latent correlations between bias, activation, and recognition performance.
- We propose InsideBias, a novel bias detection method based on the analysis of the filters activation of deep networks. InsideBias allows to detect biased models with very few samples (only 15 in our experiments), which makes it very useful for algorithm auditing and discrimination-aware machine learning.

The rest of the paper is structured as follows: Section II summarizes related works in this area. Section III introduces the formulation of the problem and the method proposed in this work. Section IV presents the experimental framework including database, models, and experimental protocol. Section V analyzes experimentally how biased different kinds of training affect the models, and presents the results obtained by the proposed bias detection method InsideBias. Finally, Section VI will summarize the main conclusions.

II. RELATED WORK

A. Demographic biases in biometrics and AI at large

The study carried out in [20] examined three commercial face detection algorithms. It revealed the discriminatory potential of these technologies and attracted the interest of the academia and industry, reaching widespread impact even in mass media. This presence in the general press comes with a risk: possible misinterpretation due to excessive generalization from the particular experiments reported in that paper (based on three particular face detection systems) to face biometrics in general, and AI at large.

The existence of undesired demographic bias and algorithmic discrimination in AI depend heavily on many factors such as: learning architecture, training strategy, target problem, and performance criteria [21]. The present work, as others recently [17], generates a better understanding of such factors: 1) as input knowledge for more informed bias analyses, and 2) to generate tools to deal with such undesired biases in practical problems.

As a representative example in this line of work examining demographic biases in AI, Nagpal et al. conducted a series of experiments to verify if deep neural networks in facial recognition systems encode some type of race-specific information

[7], and found that in models trained with different races, different discriminative regions contribute to the decision.

Kleinberg et al. rightly point out the difference between the training of the algorithm and the application of the algorithm [22]. This difference is evident in [3] where the same algorithm performed worse for dark-skinned people than for light-skinned people, given images from some cameras, but performed better for images from other cameras.

Turning to the specific case of face recognition, the work [14] proves that bias is not linked exclusively to a demographic factor. Moreover, it discusses how sensational headlines written by non-expert people skew the information around biases in AI.

B. Looking inside Neural Networks

As soon as the rebirth of Neural Networks happened in the past decade, researchers started trying to understand the representations learned by the models.

Erhan et al. proposed an approach to visualize the hidden layers [23]. Zeiler and Fergus applied a deconvolution algorithm to see the activity within the model [19], and Simonyan et al. generated the representative image of a class by maximizing the class scores [24]. Yosinski et al. visualized the activations of each neuron when processing an image [25]. Selvaraju et al. introduced an algorithm that visually highlights a networks decision by computing the gradient of the class score with respect to the input image [26]. In a similar line of work, Nguyen et al. created synthetic images that maximally activated each neuron [27], and Olah et al. explored which neurons are activated in different regions of the image [28, 29].

In addition, there are other variants and improvements of the methods indicated above, like the ones that identify characteristics encoded by the network relevant to the task [30], or other ways to intervene certain neurons in order to see the effect they have [31].

Inspired by the literature, in the present work we look at the raw activations of the neurons in presence of demographic biases in gender classification algorithms.

III. MEASURING BIAS IN DEEP NETWORKS: INSIDEBIAS

A. Formulation of the problem

Lets begin with notation and preliminary definitions. Assume \mathbf{I} is an input sample (e.g. face image) of an individual. That sample \mathbf{I} is assumed to be useful for task T , e.g., face authentication or gender recognition. That sample is part of a given dataset \mathcal{D} (collection of multiple samples from multiple subjects) used to train a model defined by its parameters \mathbf{w} . We also assume that there is a goodness criterion G_T on that task T maximizing some performance function f_T in the given dataset \mathcal{D} in the form:

$$G_T(\mathcal{D}) = \max_{\mathbf{w}} f_T(\mathcal{D}, \mathbf{w}) \quad (1)$$

On the other hand, the individuals in \mathcal{D} can be classified according to two demographic criteria (without loss of generality, we can have more criteria): $d = 1 \equiv \text{Gender} \in$

$\{Male, Female\}$ and $d = 2 \equiv Ethnicity \in \{A, B, C\}$. We assume that all classes are well represented in dataset \mathcal{D} , i.e., the number of samples of each class for all criteria in \mathcal{D} is significant. $\mathcal{D}_d^k \in \mathcal{D}$ represents all the samples corresponding to class k of demographic criterion d .

In our experiments, the goodness criterion $G_T(\mathcal{D})$ was defined as the performance of a gender recognition algorithm ($T = Gender\ Recognition$). During the experiments, we study how the criterion $d = 1 \equiv Ethnicity$ affects the internals of an algorithm focused on recognition of a different criterion $d = 2 \equiv Gender$.

B. Bias estimation with InsideBias

While most of the literature is focused on estimating bias through performance between different datasets [17], with InsideBias we propose a novel approach based on the activation levels¹ within the network for different datasets \mathcal{D}_d^k from different demographic groups.

Without loss of generality, we present InsideBias for Convolutional Neural Networks (CNNs). Similar ideas are extensible to other neural learning architectures. In a convolutional layer of a CNN, the previous layers feature maps are convolved with the filters (also known as kernels) and put through the activation function to form the output feature map. The output $\mathbf{A}^{[l]}$ of layer l consists of $m^{[l]}$ feature maps of size $n_1^{[l]} \times n_2^{[l]}$, where $m^{[l]}$ is the number of filters at layer l . The i^{th} feature map in layer l denoted as $\mathbf{A}_i^{[l]}$ is computed as:

$$\mathbf{A}_i^{[l]} = g^{[l]} \left(\sum_{j=1}^{m^{[l-1]}} \mathbf{f}_{ij}^{[l]} * \mathbf{A}_j^{[l-1]} + \mathbf{b}_i^{[l]} \right) \quad (2)$$

where $g^{[l]}$ denotes the activation function of the l^{th} layer, $*$ is the convolutional operator, $\mathbf{b}_i^{[l]}$ is a bias vector at layer l for the i^{th} feature map, and $\mathbf{f}_{ij}^{[l]}$ is the filter connecting the j^{th} feature map in layer $(l-1)$ with i^{th} feature map in layer l . The average activation of the i^{th} feature map at layer l is calculated as:

$$\overline{A_i^{[l]}} = \frac{1}{n_1^{[l]} \cdot n_2^{[l]}} \sum_{x=1}^{n_1^{[l]}} \sum_{y=1}^{n_2^{[l]}} A_i^{[l]}(x, y) \quad (3)$$

The activation, $\lambda^{[l]}$, is calculated as the maximum of $\overline{A_i^{[l]}}$ for all feature maps in the layer l :

$$\lambda^{[l]} = \max_i \left(\overline{A_i^{[l]}} \right) \quad (4)$$

which can be normalized across layers:

$$\lambda'^{[l]} = \frac{\lambda^{[l]}}{\max_l \lambda^{[l]}} \quad (5)$$

The *Activation Ratio* $\Lambda_d^{[l]}$ for demographic criterion d (e.g., *Ethnicity* in our experiments) is then calculated as the ratio

¹We refer to activation level as the output of the activation function of each neuron.



Fig. 2. Example images for the demographic **Groups (A, B and C)** used in our experiments.

between the activation obtained for the group with the lowest $\lambda^{[l]}$ and the group with the highest $\lambda^{[l]}$:

$$\Lambda_d^{[l]} = \frac{\min_k \lambda^{[l]}(\mathcal{D}_d^k)}{\max_k \lambda^{[l]}(\mathcal{D}_d^k)} \quad (6)$$

InsideBias uses this *Activation Ratio* to detect biased models. A model will be considered biased if the *Activation Ratio* is smaller than a threshold τ . When analyzing the bias in this way we recommend looking at the final layers, similar to the initial example in Fig. 1.

IV. EXPERIMENTAL FRAMEWORK

We start our bias experiments by studying how ethnic attributes influence the gender learning process. For that we trained two architectures for gender classification with different ethnic groups (biased training data) and with all the groups together (unbiased training data).

A. Database

In our experiments we used the DiveFace dataset [32]. DiveFace contains annotations equally distributed among six classes related to gender and ethnicity. There are 24K identities (4K per class) and 3 images per identity for a total number of images equal to 72K. Users are grouped according to their gender (male or female) and three categories related with ethnic physical characteristics:

- **Group A:** people with ancestral origin in Japan, China, Korea, and other countries in that region.
- **Group B:** people with ancestral origins in Sub-Saharan Africa, India, Bangladesh, Bhutan, among others.
- **Group C:** people with ancestral origins in Europe, North-America, and Latin-America (with European origin).

Fig. 2 shows 15 face images examples from the three ethnic groups of DiveFace. Note that all images show similar pose, illumination, and quality. These images obtain very high confidence values when used in gender recognition algorithms (i.e. confidence scores greater than 99%).

Note that these are heterogeneous groups that include people of different ethnicities. We are aware of the limitations of grouping all human ethnic origins into only three categories.

TABLE I

ACCURACY (%) IN GENDER CLASSIFICATION FOR NETWORK 1 AND 2 FOR EACH OF THE THREE DEMOGRAPHIC GROUPS. EACH LINE INDICATES A MODEL. THE PROTOCOL COLUMN INDICATES THE MODEL AND ETHNIC GROUPS EMPLOYED TO TRAIN, THE GROUP COLUMNS INDICATE THE TESTING GROUPS, AND THE OTHER COLUMNS: THE AVERAGE ACCURACY ACROSS GRUPS (AVG), STANDARD DEVIATION (STD) (LOWER MEANS FAIRER), AND SKEWED ERROR RATIO = (max EER)/(min EER) (1 IS FAIREST).

NETWORK 1 (CNN architecture)						
Protocol (<i>Training Groups</i>)	Group A	Group B	Group C	Avg	Std	SER
Biased (A)	95.01	89.33	90.44	91.59	2.46	2.14
Biased (B)	91.93	96.06	93.97	93.99	1.69	2.05
Biased (C)	78.58	87.82	94.33	86.91	6.46	3.78
Unbiased (A/3 + B/3 + C/3)	94.84	95.69	95.28	95.27	0.34	1.20
Unbiased+ (A + B + C)	96.47	96.76	97.54	96.92	0.45	1.43

NETWORK 2 (ResNet architecture)						
Protocol (<i>Training Groups</i>)	Group A	Group B	Group C	Avg	Std	SER
Biased (A)	95.92	91.10	91.75	92.92	2.14	2.18
Biased (B)	91.12	97.30	93.07	93.83	2.58	3.29
Biased (C)	88.96	94.80	97.08	93.61	3.42	3.78
Unbiased (A/3 + B/3 + C/3)	95.50	95.35	96.11	95.65	0.33	1.19
Unbiased+ (A + B + C)	97.47	97.44	98.17	97.69	0.34	1.40

According to studies, there are more than 5K ethnic groups in the world. We have classified them into only three groups in order to maximize differences between classes. Automatic classification algorithms based on these three categories show performances of up to 98% accuracy [6].

B. Learning architectures

We employed two popular state-of-the-art image recognition architectures based on Convolutional and Residual layers. These architectures have been chosen as examples of standard models employed in face attribute detection algorithms [33, 34]:

Network 1 (CNN architecture): The network is composed of eight convolutional layers followed by two fully connected layers with dropout. We use the ReLU (Rectified Linear Unit) activation function in all hidden layers, and a softmax activation function for the output layer (with two output units). After every two convolutions there is a maxpooling layer with a filter size of 2×2 . The three first convolutional layers have 32 filters, the two following convolutional layers have 64 filters, then two of 128 filters and the last convolutional layer has 256 filters. Each convolution is followed by a batch normalization and a ReLU activation function, and its filters are of size 3×3 and stride 1. This network comprises more than 660K parameters and its input is 120×120 .

Network 2 (ResNet architecture): The network consists of three building blocks and a fully connected layer with softmax activation for the output layer (with two output units).

The first building block has a convolutional layer with 32 filters of size 7×7 , and stride 2, followed by a 3×3 max pool of stride 2. The second and third building blocks are integrated by identity blocks and convolutional blocks. An identity block

is a series of three convolutions with a shortcut connection that bypasses the input of the identity block and jumps to the output of the third convolution of the block. A convolutional block is an identity block whose shortcut performs a convolution.

The second building block has a convolutional block (3 consecutive convolution layers with a set of 32, 32, and 128 filters of size 1×1 , 3×3 , and 1×1 , respectively), a convolutional layer shortcut (128 filters of 1×1), and two identity blocks with the same consecutive convolutional layers as the convolutional block but without the skipped connection.

The third building block has a convolutional block like the previous convolutional block but with 64, 64, and 256 filters per convolutional layer; and three identity blocks with the same series of filters per convolution. Each convolution is followed by a batch normalization and a ReLU activation function. This network comprises more than 370K parameters and its input is 120×120 .

C. Experimental protocol

We have trained five models of each of the two chosen learning architectures, according to three different experimental protocols:

- *Biased Models:* the models in this experiment are trained with 18K images of only one ethnic group (9K each, women and men). This experiment is repeated 3 times for each of the ethnic groups. Therefore, 3 independent models per network architecture are trained.
- *Unbiased Model* (trained with limited data): the models in this experiment are trained with 18K images (same number of images than biased models), 6K from each ethnic group, divided in half between men and women.

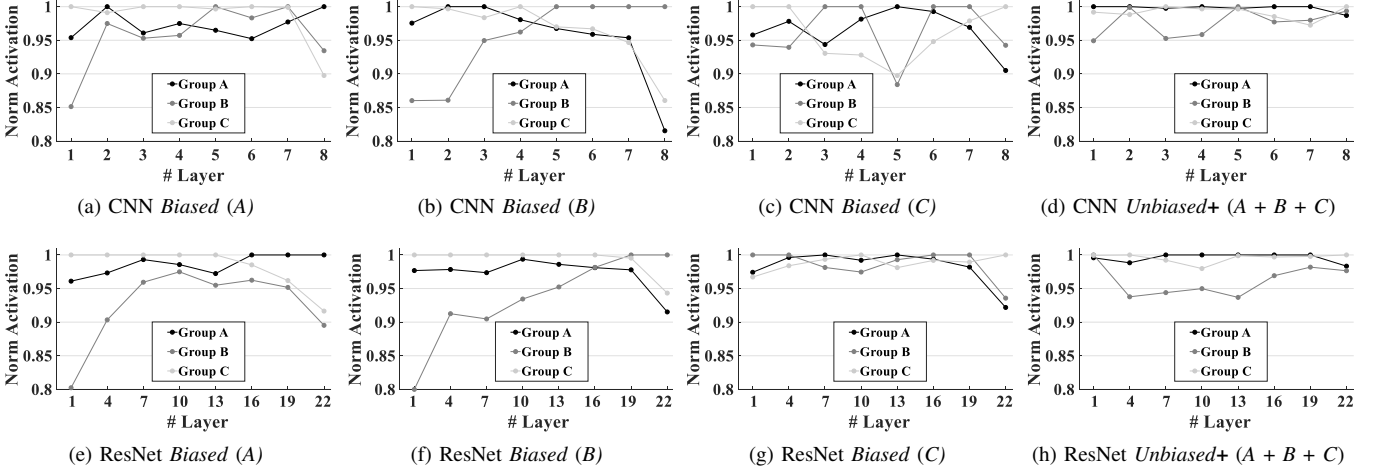


Fig. 3. Normalized activation λ' observed in **testing** (18K images) for the three demographic **Groups (A, B and C)** of the different *trained models: Biased Model (A, B and C)* and *Unbiased Model+ (A + B + C)*. The top row shows the activations of *Network 1 (CNN)* and the bottom row plots the activations of *Network 2 (ResNet)*. The CNN model has only 8 convolutional layers while ResNet model has 22 (only the main ones appear).

- *Unbiased Model Plus (+)*: the models in this experiment are trained with 54K images (three times more data than previous models), 18K from each ethnic group, divided in half between men and women.

All models are evaluated with 18K images distributed equally among all three ethnic groups. None of the validation users have been used for training; i.e., it is an independent set.

V. EXPERIMENTAL RESULTS

A. Role of the biased data

Table I shows the results of the experiments described in Section IV-C, performed on *Networks 1* and *2*, respectively (see Section IV-B). The results show that the models trained using data from a single ethnic group perform better for this group (*Biased Models*). These results suggest that the ethnic features affect the performance of gender recognition based on the two popular network architectures evaluated. The learned parameters \mathbf{w} of a model trained with one ethnic group (for example ethnic group $k = 1 \equiv \text{Asian}$) do not generalize in the best possible way for other groups, with a clear drop in performance between testing groups for both networks, i.e., using the notation introduced in Section III-A: for the network \mathbf{w}^* trained for $T = \text{Gender classification}$ by maximizing the goodness criterion G_T (see Equation 1), we observe that $G_T(\mathcal{D}_{\text{Ethnicity}}^{\text{Asian}}) \gg G_T(\mathcal{D}_{\text{Ethnicity}}^{\text{African}})$ and $G_T(\mathcal{D}_{\text{Ethnicity}}^{\text{Caucasian}})$.

The inclusion of heterogeneous data in training (*Unbiased Models*) reduces the performance gap between testing groups and improves the overall accuracy (Avg in Table II). However, the performance achieved by the models trained with heterogeneous but limited data (*Unbiased Model*: same number of training samples than biased models) does not improve the best performance achieved by each of the *Biased Models* trained using data from one ethnic group. If the model is trained with 3 times more data equally distributed across the three groups (*Unbiased+ Model*), then we observe both: an improvement of the overall accuracy and a

reduction of the performance gap between ethnic groups, i.e. $G_{\text{Gender}}(\mathcal{D}_{\text{Ethnicity}}^{\text{Asian}}) \approx G_{\text{Gender}}(\mathcal{D}_{\text{Ethnicity}}^{\text{African}}) \approx G_{\text{Gender}}(\mathcal{D}_{\text{Ethnicity}}^{\text{Caucasian}})$. These findings indicate that quantity and heterogeneity of training data help to improve the performance and fairness of these networks.

B. InsideBias: Intuition of the activation as a bias estimator

Convolutional Neural Networks are composed by a large number of stacked filters. These filters are trained to extract the richest information for a predefined task (e.g. gender recognition). These filters are activated as an input (eg. an image) goes through the net. Stronger activations are usually related to the detection of highly discriminant features [19]. The filters are usually different between networks trained differently, even if the networks have the same architecture, and even if they have been trained with the same data. E.g. if the initialization for solving Equation 1 iteratively is different, as the space of solutions is very wide [35], the solution of that Equation will typically be a local minimum depending on the particular training configuration.

Fig. 3 shows the *Normalized Activation* from Equation 5 of the different networks for each demographic group. Fig. 3 shows that the activations obtained for the *Unbiased Model+* (trained with 54K images from the three ethnic groups) have the lowest differences between ethnic groups in testing. As we can see in the activation curves per layer for the *Biased Models*, the differences in the activation between privileged and underprivileged groups are not homogeneous across layers. The curves suggest greater activation differences between testing groups in this case (*Biased Models*) in the last layers of the networks.

We also see in Fig. 3 in the first layers that testing **Group B** gets considerably less activation than the other two groups (even in the models trained with this group, see 3b and 3f), which tells us that this group has less activation for layers extracting low level features (e.g. shape, texture, and colors).

However, this lower activation in the first layers does not necessarily imply a low performance (as seen in Table I). The low activation in the first layers is compensated with high activation in the last layers which are related with high level features close to the task T (i.e. gender recognition in our experiments).

C. InsideBias: Detecting bias with very few samples

The activations presented in Fig. 3 showed the direct relationship between bias and activations over 18K images, 2 learning architectures, and 5 models trained according to different biased and unbiased dataset. Next experiments will investigate how InsideBias performs for bias detection using a small set of test samples.

Table II shows the average classification scores and the *Activation Ratio* defined in Equation 6 (l = last layer) obtained with the different considered models (Biased and Unbiased) trained for gender classification and tested with the 15 face images shown in Fig. 2. The results show how activations are correlated with biases even if the classification scores show almost no differences between biased and unbiased models. For Unbiased models an *Activation Ratio* close to one reveals a similar activation pattern for all demographic groups tested (i.e. $\lambda^{[l]}(\mathcal{D}_{Ethnicity}^{Asian}) \approx \lambda^{[l]}(\mathcal{D}_{Ethnicity}^{African}) \approx \lambda^{[l]}(\mathcal{D}_{Ethnicity}^{Caucasian})$). In contrast, the Biased models show lower *Activation Ratio*, which means higher differences between activation patterns from privileged and underprivileged demographic groups (i.e. $\lambda^{[l]}(\mathcal{D}_{Ethnicity}^{Privileged}) > \lambda^{[l]}(\mathcal{D}_{Ethnicity}^{Underprivileged})$).

These results suggest that even if the network was trained only for gender recognition, the activation level of the filters is highly sensitive to the ethnic attributes. The proposed method for bias detection in deep networks, InsideBias, consists of measuring that sensitivity with the *Activation Ratio* $\Lambda_d^{[l]}$ defined in Equation 6 and comparing it to a threshold τ .

The main advantage of this method for the analysis of bias with respect to a performance-based evaluation is that the differences are examined in terms of model behavior. Images of Fig. 2 obtained good performance (over 99.99% confidence score even in biased models) but showed clearly different activation patterns λ . Bias analysis based on performance require large datasets, and using the proposed *Activation Ratio*, few images may be enough to detect biased models.

In this work we do not underestimate the performance as a good instrument for analyzing bias in deep networks. We propose to include activation as an additional evidence [36], which is specially useful when only very few samples are available for bias analysis.

VI. CONCLUSIONS

In this work we presented a preliminary analysis of how biased data affect the learning processes of deep neural network architectures in terms of activation level. We showed how ethnic attributes affect the learning process of gender classifiers. We evaluated these differences in terms of filter activation, besides performance, and the results showed how the biases are encoded heavily in the last layers of the models.

TABLE II
AVERAGE GENDER CONFIDENCE SCORES S AND ACTIVATION RATIOS $\Lambda_d^{[l]}$ OBTAINED BY THE BIASED AND UNBIASED MODELS TESTED FOR THE 15 IMAGES OF FIG. 2. l = LAST LAYER. 1 IS 100% CONFIDENCE ABOUT THE TRUE GENDER ATTRIBUTE IN THE IMAGE.

Model (Training)		Test Group			$\Lambda_d^{[l]}$
		A	B	C	
CNN-Biased (A)	S	0.999	1.000	0.999	-
	$\lambda^{[l]}$	2.78	3.15	2.59	0.82
CNN-Biased (B)	S	0.999	1.000	1.000	-
	$\lambda^{[l]}$	2.37	2.75	2.59	0.86
CNN-Biased (C)	S	0.999	0.997	1.000	-
	$\lambda^{[l]}$	2.43	2.35	2.81	0.83
CNN-Unbiased (A/3 + B/3 + C/3)	S	1.000	1.000	1.000	-
	$\lambda^{[l]}$	2.49	2.67	2.51	0.93
CNN-Unbiased+ (A + B + C)	S	1.000	1.000	1.000	-
	$\lambda^{[l]}$	2.68	2.82	2.92	0.92
ResNet-Biased (A)	S	1.000	1.000	1.000	-
	$\lambda^{[l]}$	2.41	2.20	2.14	0.88
ResNet-Biased (B)	S	0.999	1.000	1.000	-
	$\lambda^{[l]}$	2.34	2.88	2.76	0.81
ResNet-Biased (C)	S	1.00	1.000	1.000	-
	$\lambda^{[l]}$	2.03	2.11	2.29	0.89
ResNet-Unbiased (A/3 + B/3 + C/3)	S	0.999	0.999	0.999	-
	$\lambda^{[l]}$	2.33	2.32	2.34	0.99
ResNet-Unbiased+ (A + B + C)	S	1.000	1.000	1.000	-
	$\lambda^{[l]}$	2.34	2.19	2.36	0.93

This activation reveals behaviors usually hidden during the learning process. We also evaluated different training strategies that suggest to what extent biases can be reduced if the whole network is trained using a heterogeneous dataset.

We finally propose a novel method, InsideBias, to detect bias through layer activations. InsideBias has two major advantages with respect to detection based on performance differences across demographic groups: 1) it does not require many samples (we showed that biased behaviors can be detected with only 15 images), and 2) InsideBias can give an indication of the bias in the model using only good samples correctly recognized (even with the highest confidence).

VII. ACKNOWLEDGMENTS

This work has been supported by projects BIBECA (RTI2018-101248-B-I00 MINECO/FEDER), TRESPASS (MSCA-ITN-2019-860813), PRIMA (MSCA-ITN-2019-860315), and Accenture. I. Serna is supported by a research fellowship from the Spanish CAM.

REFERENCES

- [1] P. Stone, R. Brooks, E. Brynjolfsson, R. Calo, O. Etzioni, G. Hager, J. Hirschberg, S. Kalyanakrishnan, E. Kamar, S. Kraus *et al.*, “Artificial Intelligence and Life in 2030,” *One Hundred Year Study on Artificial Intelligence: Report of the 2015-2016 Study Panel*, p. 52, 2016.
- [2] C. Szegedy, W. Zaremba, I. Sutskever, J. B. Estrach, D. Erhan, I. Goodfellow, and R. Fergus, “Intriguing Properties of Neural Networks,” in *International Conference on Learning Representations (ICLR)*, Banff, Canada, 2014.
- [3] C. M. Cook, J. J. Howard, Y. B. Sirotin, J. L. Tipton, and A. R. Vemury, “Demographic Effects in Facial Recognition and Their Dependence on Image Acquisition: An Evaluation of Eleven Commercial Systems,” *IEEE Transactions on Biometrics, Behavior, and Identity Science*, vol. 1, no. 1, pp. 32–41, 2019.
- [4] J. A. Buolamwini, “Gender Shades: Intersectional Phenotypic and Demographic Evaluation of Face Datasets and Gender Classifiers,” Ph.D. dissertation, Massachusetts Institute of Technology, 2017.
- [5] M. Alvi, A. Zisserman, and C. Nellåker, “Turning a Blind Eye: Explicit Removal of Biases and Variation from Deep Neural Network embeddings,” in *European Conference on Computer Vision (ECCV)*, Munich, Germany, 2018.
- [6] A. Acien, A. Morales, R. Vera-Rodriguez, I. Bartolome, and J. Fierrez, “Measuring the Gender and Ethnicity Bias in Deep Models for Face Recognition,” in *Iberoamerican Congress on Pattern Recognition (IAPR)*. Madrid, Spain: Springer, 2018, pp. 584–593.
- [7] S. Nagpal, M. Singh, R. Singh, M. Vatsa, and N. Ratha, “Deep Learning for Face Recognition: Pride or Prejudiced?” *arXiv:1904.01219*, 2019.
- [8] P. J. Phillips, F. Jiang, A. Narvekar, J. Ayyad, and A. J. O’Toole, “An Other-Race Effect for Face Recognition Algorithms,” *ACM Transactions on Applied Perception*, vol. 8, no. 2, p. 14, 2011.
- [9] A. J. O’Toole, P. J. Phillips, X. An, and J. Dunlop, “Demographic Effects on Estimates of Automatic Face Recognition Performance,” *Image and Vision Computing*, vol. 30, no. 3, pp. 169–176, 2012.
- [10] B. F. Klare, M. J. Burge, J. C. Klontz, R. W. V. Bruegge, and A. K. Jain, “Face Recognition Performance: Role of Demographic Information,” *IEEE Transactions on Information Forensics and Security*, vol. 7, no. 6, pp. 1789–1801, 2012.
- [11] H. Han, C. Otto, X. Liu, and A. K. Jain, “Demographic Estimation from Face Images: Human vs. Machine Performance,” *IEEE Transactions on Pattern Analysis and Machine Intelligence*, vol. 37, no. 6, pp. 1148–1161, 2015.
- [12] P. J. Grother, M. L. Ngan, and K. K. Hanaoka, *Ongoing Face Recognition Vendor Test (FRVT) Part 2: Identification*, ser. NIST Internal Report. U.S. Department of Commerce, National Institute of Standards and Technology, 2018.
- [13] —, *Ongoing Face Recognition Vendor Test (FRVT) Part 3: Demographic Effects*, ser. NIST Internal Report. U.S. Department of Commerce, National Institute of Standards and Technology, 2019.
- [14] J. J. Howard, Y. Sirotin, and A. Vemury, “The Effect of Broad and Specific Demographic Homogeneity on the Imposter Distributions and False Match Rates in Face Recognition Algorithm Performance,” in *International Conference on Biometrics Theory, Applications and Systems (BTAS)*. Tampa, Florida, USA: IEEE, 2019.
- [15] I. Hupont and C. Fernandez, “DemogPairs: Quantifying the Impact of Demographic Imbalance in Deep Face Recognition,” in *International Conference on Automatic Face & Gesture Recognition (FG)*. Lille, France: IEEE, 2019.
- [16] B. Lu, J.-C. Chen, C. D. Castillo, and R. Chellappa, “An Experimental Evaluation of Covariates Effects on Unconstrained Face Verification,” *IEEE Transactions on Biometrics, Behavior, and Identity Science*, vol. 1, no. 1, pp. 42–55, 2019.
- [17] P. Drozdowski, C. Rathgeb, A. Dantcheva, N. Damer, and C. Busch, “Demographic Bias in Biometrics: A Survey on an Emerging Challenge,” *arXiv:2003.02488*, 2020.
- [18] J. Deng, W. Dong, R. Socher, L.-J. Li, K. Li, and L. Fei-Fei, “Imagenet: A Large-Scale Hierarchical Image Database,” in *Conference on Computer Vision and Pattern Recognition (CVPR)*. Miami, Florida, USA: IEEE, 2009, pp. 248–255.
- [19] M. D. Zeiler and R. Fergus, “Visualizing and Understanding Convolutional Networks,” in *European Conference on Computer Vision (ECCV)*. Zurich, Switzerland: Springer, 2014, pp. 818–833.
- [20] J. Buolamwini and T. Gebru, “Gender Shades: Intersectional Accuracy Disparities in Commercial Gender Classification,” in *Conference on Fairness, Accountability and Transparency*, ser. Proceedings of Machine Learning Research, S. A. Friedler and C. Wilson, Eds., vol. 81, New York, NY, USA, 23–24 Feb 2018, pp. 77–91.
- [21] I. Serna, A. Morales, J. Fierrez, N. Cebrian, M. Obradovich, and I. Rahwan, “Algorithmic Discrimination: Formulation and Exploration in Deep Learning-based Face Biometrics,” in *AAAI Workshop on Artificial Intelligence Safety (SafeAI)*, New York, NY, USA, 2020.
- [22] J. Kleinberg, J. Ludwig, S. Mullainathan, and C. R. Sunstein, “Discrimination in the Age of Algorithms,” *Journal of Legal Analysis*, vol. 10, pp. 113–174, 04 2019.
- [23] D. Erhan, Y. Bengio, A. Courville, and P. Vincent, “Visualizing Higher-Layer Features of a Deep Network,” University of Montreal, Tech. Rep. 1341, Jun. 2009.
- [24] K. Simonyan, A. Vedaldi, and A. Zisserman, “Deep Inside Convolutional Networks: Visualising Image Classification Models and Saliency Maps,” in *International Conference on Learning Representations (ICLR) Workshop*, Banff, Canada, 2014.

- [25] J. Yosinski, J. Clune, A. Nguyen, T. Fuchs, and H. Lipson, "Understanding Neural Networks Through Deep Visualization," in *International Conference on Machine Learning (ICML) Deep Learning Workshop*, Lille, France, 2015.
- [26] R. R. Selvaraju, M. Cogswell, A. Das, R. Vedantam, D. Parikh, and D. Batra, "Grad-CAM: Visual Explanations from Deep Networks Via Gradient-Based Localization," in *International Conference on Computer Vision (CVPR)*. Honolulu, Hawaii, USA: IEEE, 2017, pp. 618–626.
- [27] A. Nguyen, J. Yosinski, and J. Clune, "Multifaceted Feature Visualization: Uncovering the Different Types of Features Learned by Each Neuron in Deep Neural Networks," in *International Conference on Machine Learning (ICML) Deep Learning Workshop*, New York, NY, USA, 2016.
- [28] C. Olah, A. Satyanarayan, I. Johnson, S. Carter, L. Schubert, K. Ye, and A. Mordvintsev, "The Building Blocks of Interpretability," *Distill*, vol. 3, no. 3, 2018.
- [29] C. Olah, A. Mordvintsev, and L. Schubert, "Feature Visualization," *Distill*, vol. 2, no. 11, 2017.
- [30] J. Oramas, K. Wang, and T. Tuytelaars, "Visual Explanation by Interpretation: Improving Visual Feedback Capabilities of Deep Neural Networks," in *International Conference on Learning Representations (ICLR)*, New Orleans, Louisiana, USA, 2019.
- [31] B. Zhou, Y. Sun, D. Bau, and A. Torralba, "Revisiting the Importance of Individual Units in CNNs via Ablation," *arXiv:1806.02891*, 2018.
- [32] A. Morales, J. Fierrez, and R. Vera-Rodriguez, "SensitiveNets: Learning Agnostic Representations with Application to Face Recognition," *arXiv:1902.00334*, 2019.
- [33] R. Ranjan, S. Sankaranarayanan, A. Bansal, N. Bodla, J.-C. Chen, V. M. Patel, C. D. Castillo, and R. Chellappa, "Deep Learning for Understanding Faces: Machines May Be Just as Good, or Better, than Humans," *IEEE Signal Processing Magazine*, vol. 35, no. 1, pp. 66–83, 2018.
- [34] E. Gonzalez-Sosa, J. Fierrez, R. Vera-Rodriguez, and F. Alonso-Fernandez, "Facial Soft Biometrics for Recognition in the Wild: Recent Works, Annotation and COTS Evaluation," *IEEE Trans. on Information Forensics and Security*, vol. 13, no. 8, pp. 2001–2014, August 2018.
- [35] Y. LeCun, Y. Bengio, and G. Hinton, "Deep Learning," *Nature*, vol. 521, no. 7553, pp. 436–444, 2015.
- [36] J. Fierrez, A. Morales, R. Vera-Rodriguez, and D. Camacho, "Multiple Classifiers in Biometrics. Part 2: Trends and Challenges," *Information Fusion*, vol. 44, pp. 103–112, November 2018.